Use of innovative, cross-disciplinary in vitro, in silico and in vivo approaches to characterize the metabolism of chloro-alpha-pyrrolidinovalerophenone (4-Cl-PVP)

Romain Pelletier, Brendan Le Daré, Pierre-Jean Ferron,, Diane Le Bouedec, Angéline Kernalléguen, Isabelle Morel, Thomas Gicquel

Use of innovative, cross-disciplinary *in vitro, in silico* and *in vivo* approaches to characterize the metabolism of chloro-alpha-pyrrolidinovalerophenone (4-Cl-PVP)

Romain Pelletier[a,b], Brendan Le Daré[b,c] , Pierre-Jean Ferron[a], Diane Le Bouedec[b], Angéline Kernalléguen[a], Isabelle Morel[a, b], Thomas Gicquel[a, b]

[a]: *INSERM, Univ Rennes, INRAE, Institut NUMECAN (Nutrition, Metabolisms and Cancer) UMR_A 1341, UMR_S 1241, F-35000, Rennes, France*

[b]: *Rennes University Hospital, Clinical and Forensic Toxicology laboratory, F-35033 Rennes, France*

[c]: *Rennes University Hospital, Pharmacy, F-35033 Rennes, France*

* Correspondence to:

Romain Pelletier, PharmD

Laboratoire de toxicologie biologique et medico-légale, CHU Pontchaillou, 2 Rue Henri Le Guilloux, 35000 Rennes, France

romain.pelletier@chu-rennes.fr

Authors' ORCID :

Romain Pelletier: 0000-0002-3848-507X

Brendan Le Daré: 0000-0002-5907-2450

Pierre-Jean Ferron: 0000-0002-7417-4690

Thomas Gicquel: 0000-0002-2354-1884

Abstract

Synthetic cathinones constitute a family of new psychoactive substances, the consumption of which is increasingly worldwide. A lack of metabolic knowledge limits the detection of these compounds in cases of intoxication. Here, we used an innovative cross-disciplinary approach to study the metabolism of the newly emerging cathinone chloro-alpha-pyrrolidinovalerophenone (4-Cl-PVP).

Three complementary approaches (*in silico*, *in vitro*, and *in vivo)* were used to identify putative 4-Cl-PVP metabolites that could be used as additional consumption markers. The *in silico* approach used predictive software packages. Molecular networking was used as an innovative bioinformatics approach for re-processing high-resolution tandem mass spectrometry data acquired with both *in vitro* and *in vivo* samples. *In vitro* experiments were performed by incubating 4-Cl-PVP (20 µM) for four different durations with a metabolically competent human hepatic cell model (differentiated HepaRG cells). *In vivo* samples (blood and urine) were obtained from a patient known to have consumed 4-Cl-PVP.

The *in silico* software predicted 17 putative metabolites, and molecular networking identified 10 metabolites *in vitro*. On admission to the intensive care unit, the patient's plasma and urine 4-Cl-PVP concentrations were respectively 34.4 and 1018.6 µg/L. An *in vivo* analysis identified the presence of five additional glucuronoconjugated 4-Cl-PVP derivatives in the urine.

Our combination of a cross-disciplinary approach with molecular networking enabled the detection of 15 4-Cl-PVP metabolites, 10 of them had not previously been reported in the literature. Two metabolites appeared to be particular relevant candidate as 4-Cl-PVP consumption markers in cases of intoxication: hydroxy-4-Cl-PVP (*m/z* 282.1254) and dihydroxy-4-Cl-PVP (*m/z* 298.1204).

Keywords: new psychoactive substances, 4-Cl-PVP, metabolism, molecular networking, HepaRG Cells, *in silico*

Introduction

Drug addiction is a major public health issue and has been accentuated by the arrival of a variety of new psychoactive substances (NPS); the incidence of intoxication has increased worldwide (Miotto et al. 2013; Abuse 2020; La Maida et al. 2021). At the end of 2021, the European Monitoring Center for Drugs and Drug Addiction was monitoring 162 cathinones - the second most prevalent type of NPS, after synthetic cannabinoids (European Monitoring Centre for Drugs and Drug Addiction. 2022). Cathinones are emerging amphetamine derivatives of cathine (a compound present in the leaves of the African shrub khat) used for their euphoric and stimulating properties (Kelly 2011; Majchrzak et al. 2018). In France, these drugs are commonly used during chemsex among “men who have sex with men” (Batisse et al. 2022). However, the cathinones’ toxic effects and metabolism have not been extensively characterized, and the absence of a cathinone consumption marker hinders the detection of cases of intoxication by toxicology laboratories. This is particularly the case for 4-chloro-alpha-pyrrolidinovalerophenone (4-Cl-PVP), for which no cases of intoxication have been reported in the scientific and medical literature.

In vitro, *in vivo* and (most recently) *in silico* approaches can be used to study the metabolism of NPSs. The *in vitro* approaches include metabolic studies with human liver microsomes; this cell-free model contains membrane-bound drug metabolizing enzymes, such as cytochrome P450 (CYP) (Richeval et al. 2017; Lopes et al. 2021). In contrast, cell-based models (such as metabolically competent primary human hepatocytes (PHHs) and the differentiated HepaRG cell line) approximate physiological conditions; xenobiotics and their metabolites are thus exposed to cell barriers and intracellular components, and so the NPS’ dynamics and toxicity in liver cells can be studied (Diao and Huestis 2019; Le Daré et al. 2020b). In particular, the HepaRG cell line stably expresses CYPs and uridine glucuronyl transferases (UGTs) and so metabolizes xenobiotics in much the same way as PHHs (Aninat et al. 2006; Quesnot et al. 2018; Hugbart et al. 2020). We have previously used the HepaRG to study the metabolism of other NPSs (Richeval et al. 2017; Allard et al. 2019; Gicquel et al. 2021a). *In vivo* approaches are considered to be the “gold standard” because they feature suitable consumption markers of drug intake (depending on the matrix analyzed) and take account of the pharmacokinetic properties of the metabolites’ parent molecule. Thus, studies of NPS metabolism in human blood and

urine samples are still the most relevant (Allard et al. 2019; Gicquel et al. 2021b; Ameline et al. 2019a, b; Allibe et al. 2018; Pelletier et al. 2021).

In order to make the best use of metabolic data obtained *in vitro* and *in vivo*, bioinformatics analyses of liquid chromatography-high resolution mass spectrometry (LC-HRMS) data are becoming increasingly valuable (Seidl et al. 2022; Klingberg et al. 2022). For example, molecular networking facilitates the computational reprocessing of big data and is used increasingly in analytical and clinical toxicology labs (Allard et al. 2019, 2020; Le Daré et al. 2020b). This powerful bioinformatics tool links spectrally related molecules by comparing their fragmentation spectra and analyzing mass differences between compounds that may correspond to known biotransformation reactions; it is therefore possible to identify metabolic pathways by information propagation from a known molecule (Le Daré et al. 2020a).

Lastly, *in silico* metabolism prediction software is the most recently developed technique. It provides access to metabolic but circumvents the drawbacks of cell culture or poor sample availability. In studies of metabolism, *in silico* systems incorporate models based on (i) the quantitative structure-activity relationship, which assumes that molecules with similar structures potentially exhibit similar metabolism properties, (ii) docking potential substrates into the active site of the enzyme, or (iii) quantum mechanical calculations used to predict reactivity (Du et al. 2008; Gertrudes et al. 2012; Kazmi et al. 2019; Tyzack and Kirchmair 2019; Di Trana et al. 2021). In addition to *in vitro* and *in vivo* approaches, the *in silico* approach confirms the level of evidence required for the identification of metabolites in a simple, rapid and cost-effective manner.

The primary objective of the present study was to elucidate the metabolism of 4-Cl-PVP by applying a combination of *in vitro, in vivo* and *in silico* techniques. This innovative approach was coupled with molecular networking, in order to thoroughly explore the metabolism of this emerging NPS and to determine the chemical structures of its likely metabolites. The secondary objective was to identify putative 4-Cl-PVP additional consumption markers for use in clinical practice.

Material and methods

A CASE OF INTOXICATION WITH 4 -CL-PVP

A 49-year-old patient was admitted to the emergency department at Rennes University Hospital of (Rennes, France) with confusion and incoherent speech. The patient was known for drug abuse and schizoaffective disorders. The emergency services had observed a bag labelled “4-Cl-PVP”, an electronic cigarette liquid and 1-propionyl-lysergic acid diethylamide (1P-LSD) pills among the patient’s possessions. On admission to the intensive care unit (ICU), the patient presented with tachycardia (120 beats per minute) and arterial hypertension (140/80 mmHg). Standard laboratory assays did not reveal any cardiac, hepatic, renal, hemostatic or electrolyte disorders. Toxicological analyses of blood and urine samples were performed on admission and after 24 hours in hospital. The NPSs fluorometamphetamine (FMA), methylmethcathinone (MMC) and 4-Cl-PVP were identified in samples of the patient’s biological fluids, along with methadone (prescribed for opioid use disorder), the anxiolytic diazepam and the antipsychotic clozapine and loxapine. The patient was discharged 48 hours after admission.

MATERIAL

William's E medium was purchased from Gibco (ThermoFisher Scientific, San Jose, CA, USA). Penicillin-streptomycin was obtained from Life Technologies (Grand Island, NY, USA). Fetal bovine serum was purchased from Eurobio (Courtaboeuf, France). Glutamine was obtained from Life Technologies (Paisley, UK). Hydrocortisone hemisuccinate was purchased from SERB (Paris, France). Dimethylsulfoxide (DMSO), formic acid, ammonium acetate and insulin were obtained from Sigma-Aldrich (Saint Louis, MO, USA). LC-MS grade methanol, acetonitrile and water were obtained from Fisher Scientific UK (Loughborough, UK). The 4-Cl-PVP standard solution (1 mg/ml in methanol) was a gift from Dr Jean-Michel Gaulier (Lille University Hospital, Lille, France).

HEPARG CELL CULTURE

The HepaRG cell line (initially obtained from a liver tumor of a patient with hepatocarcinoma) was cultured as described previously (Aninat et al. 2006). Briefly, HepaRG cells were seeded at a density of 10^5 cells/well in 96-well plates and cultured for 2 weeks in William's culture medium E supplemented

with 10% fetal bovine serum, 50 U/mL penicillin, 50 µg/mL streptomycin, 5 µg/mL insulin, 2 mM glutamine, 50 µM hydrocortisone sodium hemisuccinate, and 2% DMSO. The cells were then cultured for an additional 2 weeks in the same medium supplemented with 2% DMSO, to induce cell differentiation into cholangiocyte- and hepatocyte-like cells; as described previously, these cells express liver-specific metabolic functions capable of producing phase I and II metabolites (Richeval et al. 2017; Le Daré et al. 2020b; Gicquel et al. 2021a; Ferron et al. 2021).

Cell treatment with 4-Cl-PVP

Differentiated HepaRG cells were incubated for 8, 24 or 48 hours in 100 µL of medium containing 4-Cl-PVP at three different concentrations (1, 10, and 20 µM). Cell culture supernatants were recovered, frozen at -20°C, and thawed immediately before extraction for analysis. 96-well plates were incubated in 5% CO_2 controlled atmosphere in a thermostatic chamber at 37°C, as described elsewhere (Le Daré et al. 2020b; Gicquel et al. 2021a). All *in vitro* experiments were performed in triplicate.

Sample extraction

Two hundred microliters of each sample (cell supernatant or biological fluid) were supplemented with 500 µL of methanol and 300 µL of a 0.1 mol/L zinc sulfate solution for extraction. After evaporation of the supernatant, the residue was taken up in 200 µL of mobile phase and transferred to chromatographic vials for analysis using LC-HRMS (Le Daré et al. 2020b).

4-Cl-PVP assay by LC-MS/MS

4-Cl-PVP concentrations were measured using liquid chromatography-tandem mass spectrometry (LC-MS/MS) on a Xevo TQ-XS quadrupole mass spectrometer with an electrospray ionization (ESI) source. The instrument was coupled to a Waters Acquity Class-H Plus equipped with a quaternary pump system (Waters, Milford MA, USA) and an Acquity HSS C18 column (150 × 2 mm, 1.8 µm, Waters) during 15 min. The column was held at 40°C, and the autosampler was set to 15°C. Ions were detected in multiple reaction monitoring mode. The transitions (collision energies) monitored were m/z 266.1 → 125.0 and 195.1 (24/16 eV) for 4-Cl-PVP and 242.0 → 129.0 (26 eV) for the internal standard (ketamine-d4) (Supplemental data 1).

LC-HRMS/MS ANALYSIS

LC-HRMS was performed with an UltiMate 3000 pump coupled to a Q Exactive mass spectrometer (Thermo Scientific, San Jose, CA, USA) with a heated ESI source. The non-targeted LC-HRMS/MS screening method used to build the molecular network has been described elsewhere (Le Daré et al. 2020b, 2021; Gicquel et al. 2021a; Ferron et al. 2021). Briefly, LC was performed on an Accucore Phenyl Hexyl (100 × 2.1 mm, 2.6 µm) column (Thermo Scientific) at 40°C, using an injection volume of 10 µL, an elution gradient, and a flow rate of 500 µL/min for 15 minutes. The orbitrap mass spectrometer operated in positive ESI mode, with the acquisition range of 100-700 *m/z*. Ion precursor selection was performed in "data-dependent" mode: the five most intense ions from the previous scan were selected for fragmentation ("top N of 5") (Supplemental data 2).

GENERATION OF MOLECULAR NETWORKS

The semi-quantitative approach to molecular network generation has been described elsewhere (Allard et al. 2019, 2020; Le Daré et al. 2020b; Gicquel et al. 2021a). Briefly, spectral raw data (.raw format) were converted into an open MS format (.mzXML) and then preprocessed (deconvolution, deisotoping, alignment, gap-filling, and filtering) with MZmine 2. 4.1 software (mzmine.github.io). The single .mgf output file was then loaded on the Global Natural Products Social networking (GNPS) web platform (gnps.ucsd.edu), to generate the molecular network. Nodes represented the molecules and were linked and grouped into clusters when they were spectrally close. Biotransformation reactions were identified from the mass difference between molecules. Links between nodes were created when the cosine score was greater than 0.7. The molecular network was visualized using Cytoscape 3.8.0 software (San Diego, CA, USA). Nodes were labelled with the exact protonated mass (*m/z*), and the links between nodes were labelled with the exact mass shift. A color was assigned to each concentration, and the areas of different colors in each node semi-quantitatively represented the concentrations of the corresponding compound in each condition, as described previously (Le Daré et al. 2020b; Gicquel et al. 2021a) (Supplemental data 3).

STRUCTURAL IDENTIFICATION ON THE BASIS OF THE LC-HRMS/MS DATA

The LC-HRMS/MS technique enabled mass determination to four digits after the decimal point. The main fragments provided structural information about the corresponding parent molecule. Nodes were

annotated by spectral matching using SIRIUS 4.0 software (bio.informatik.uni-jena.de/Sirius) and information propagation (identified nodes were used as starting points to identify other nodes in the same cluster), as described previously (Dührkop et al. 2019).

IN SILICO METABOLIC ANALYSES

Open-access Biotransformer 3.0 (BT3) (https://biotransformer.ca) and GLORYx (https://nerdd.univie.ac.at/gloryx/) freeware were used to compare the metabolites identified *in vivo* and *in vitro*. These programs predict the phase I and II metabolites of molecules in a .sdf file on the basis of their site of metabolism, CYP activity, and phase II metabolism rules (de Bruyn Kops et al. 2021; Wishart et al. 2022). Metabolism studies with BT3 were designed with the modules for phase I transformations (CYP 1A, 2A, 2B, 2C, 2D, 2E, and 3A4) and Phase II transformations (glucuronidation and sulfation) using « Custom Human Multi-Step Transformation (Multibio)" module. This approach also enables the prediction of the cytochrome involved in biotransformations. The GLORYx program simultaneously predicts phase I and phase II metabolites and gives a predictive score ranging from 0 to 1. Only metabolites with a predictive score greater than or equal to 0.3 were taken into consideration in the present study (Carlier et al. 2022).

Results

IN VITRO METABOLIC ANALYSES USING MOLECULAR NETWORKS

To understand the kinetics of 4-Cl-PVP's metabolism, we incubated the drug (1, 10 or 20 µM) with differentiated HepaRG cells for 0, 8, 24 or 48 hours. No cytotoxicity effects were observed under these conditions (Supplemental data 4). To increase the number of metabolites produced, the highest concentration (20 µM) was therefore chosen for *in vitro* metabolism study. Analysis of the culture supernatant at different time points provided a multimatrix molecular network that displayed the acquired MS/MS data (Figure 1). As the nodes were clustered together according to their MS/MS spectral similarities, we found a cluster in which 4-Cl-PVP was linked to structurally related compounds (Figure 1). The mass differences between nodes (shown on the links between nodes) were found to correspond to known biotransformation reactions: dehydrogenation (Δm=2.016), oxidation (Δm=15.995), oxidation + dehydrogenation (Δm=13.979), hydrolysis (Δm=18.011), oxidation and hydroxylation (Δm=29.974), and glucuronoconjugation (Δm=176.032).

Compounds structurally related to 4-Cl-PVP appeared progressively over time, with a peak concentration after 48 h of incubation. Only 4-Cl-PVP was found in the control condition (depicted in white). Three types of metabolites were observed: (i) early metabolites, detected from 8 h onwards (in pink: *m/z* 256.1106, *m/z* 280.1097, *m/z* 282.1254, *m/z* 284.1411, *m/z* 298.1204), (ii) intermediate metabolites, detected from 24 h onwards (in orange: *m/z* 238.0992, *m/z* 458.1574, *m/z* 300.1367, *m/z* 314.1153), and (iii) late metabolites detected at 48 h only (in red: *m/z* 296.1047, *m/z* 298.1206) (Figure 1).

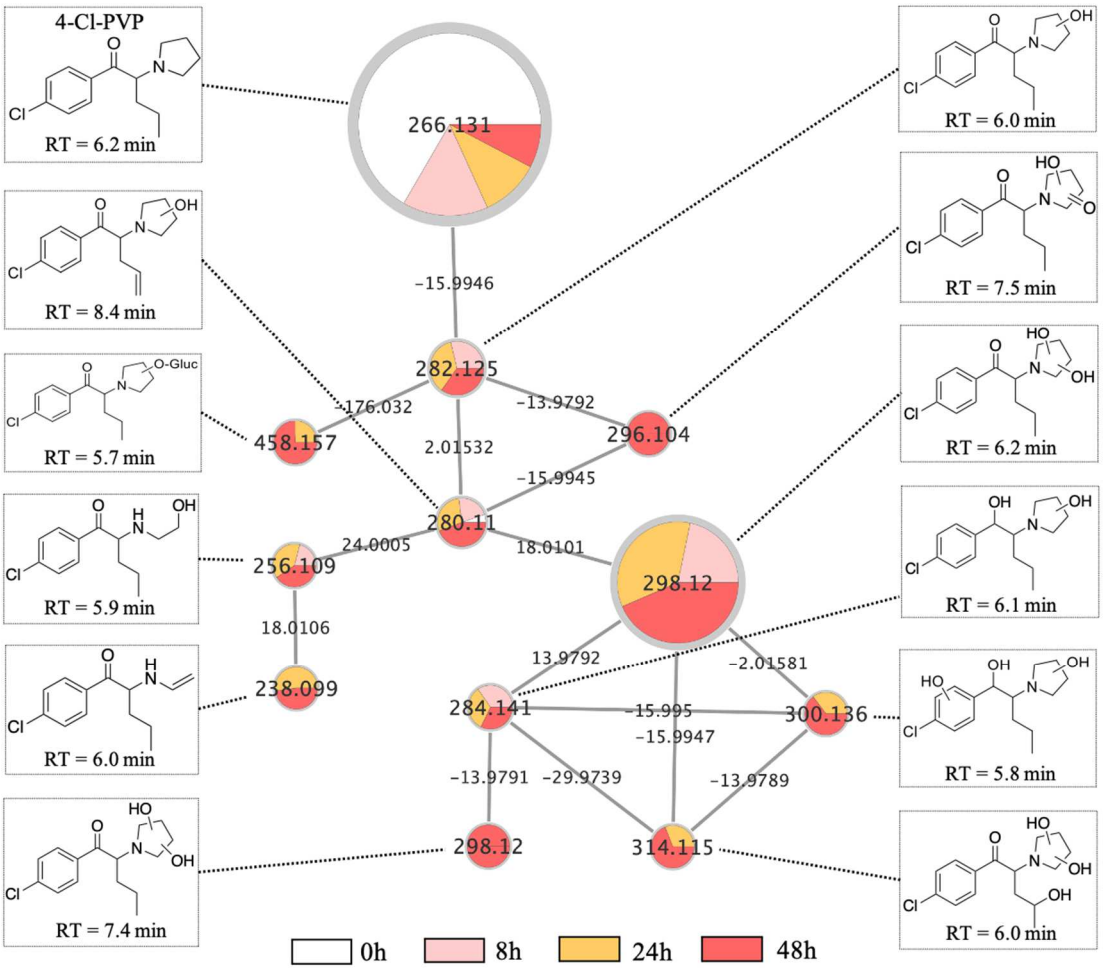

Figure 1: Visualization of in vitro 4-Cl-PVP metabolism in differentiated HepaRG cells, using molecular networking. HepaRG cells were incubated with 4-Cl-PVP (20 µM) for 0 (control), 8, 24 and 48 h: the corresponding results are depicted in white, pink, orange, and red, respectively. Nodes are labeled with the exact protonated mass (m/z), and the links are labeled with the exact mass shift. Candidate 4-Cl-PVP metabolites are linked to the corresponding nodes. RT: retention time (in minutes).

By information propagation within the molecular network and analysis of the fragmentation spectra, we were able to draw up putative chemical structures for each node (characterized by its retention time (RT)), as described previously (Le Daré et al. 2020b) (Figure 2A-D). Assessment of the fragmentation spectrum highlighted specific fragments corresponding to chemical nodes and thus enabled us to recreate the molecule's putative chemical structure. Four specific fragments of 4-Cl-PVP were identified (*m/z* 72.0821, *m/z* 125.0153, *m/z* 138.9942, and *m/z* 195.0577); this also enabled us to distinguish between isomers (such as hydroxylated compounds) in particular (Figure 2A-B). We used this approach to determine whether or not phase II biotransformation reactions (exemplified by glucuronidation) had taken place (Figure 2D).

Taken as a whole, these results (i) provided a good level of understanding of the kinetics of 4-Cl-PVP metabolism *in vitro*, (ii) suggested that compounds structurally related to 4-Cl-PVP were indeed metabolites, and (iii) confirmed that differentiated HepaRG cells constitute a relevant model for studying cathinone metabolism *in vitro* (Wagmann et al. 2020).

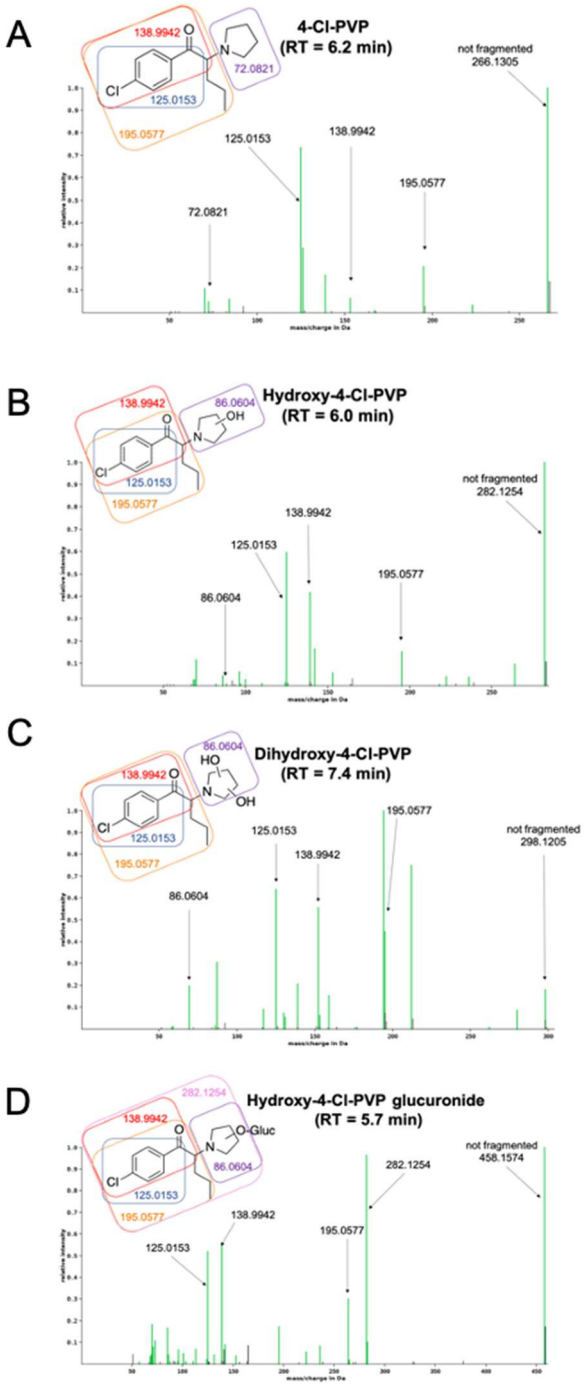

Figure 2. Structure elucidation of 4-Cl-PVP (A), Hydroxy-4-Cl-PVP (B), Dihydroxy-4-Cl-PVP (C) and Hydroxy-4-Cl-PVP glucuronide (D) using fragmentation spectrum.

METABOLITE PREDICTION USING *IN SILICO* SOFTWARE

In silico prediction of 4-Cl-PVP metabolism was performed with GLORYx and BT3. BT3 suggested 29 4-Cl-PVP metabolites, including 10 isomers with an [M+H]+ mass of 282.1254 and 6 isomers with an [M+H]+ mass of 458.1582. These metabolites correspond to the products of respectively hydroxylation and glucuronidation at different positions on 4-Cl-PVP. BT3 predict also a lot of glucuronide and sulfate deratives. BT3 is able to predicte the production of a nonspecific molecule corresponding to a furan ring with an [M+H]+ mass of 72.0821. CYP1A2 was predicted to be the main CYP involved in the metabolism of 4-Cl-PVP (Figure 3). The GLORYx software predicted five metabolites of 4-Cl-PVP including two isomers with an [M+H]+ mass of 282.1254 – again corresponding to hydroxylation of 4-Cl-PVP. Overall, the *in silico* approach generated 17 potential metabolites (Figure 3). Three of the 31 were predicted by both programs (two isomers with [M+H]+ 282.1254 and a compound with [M+H]+ 268.1468).

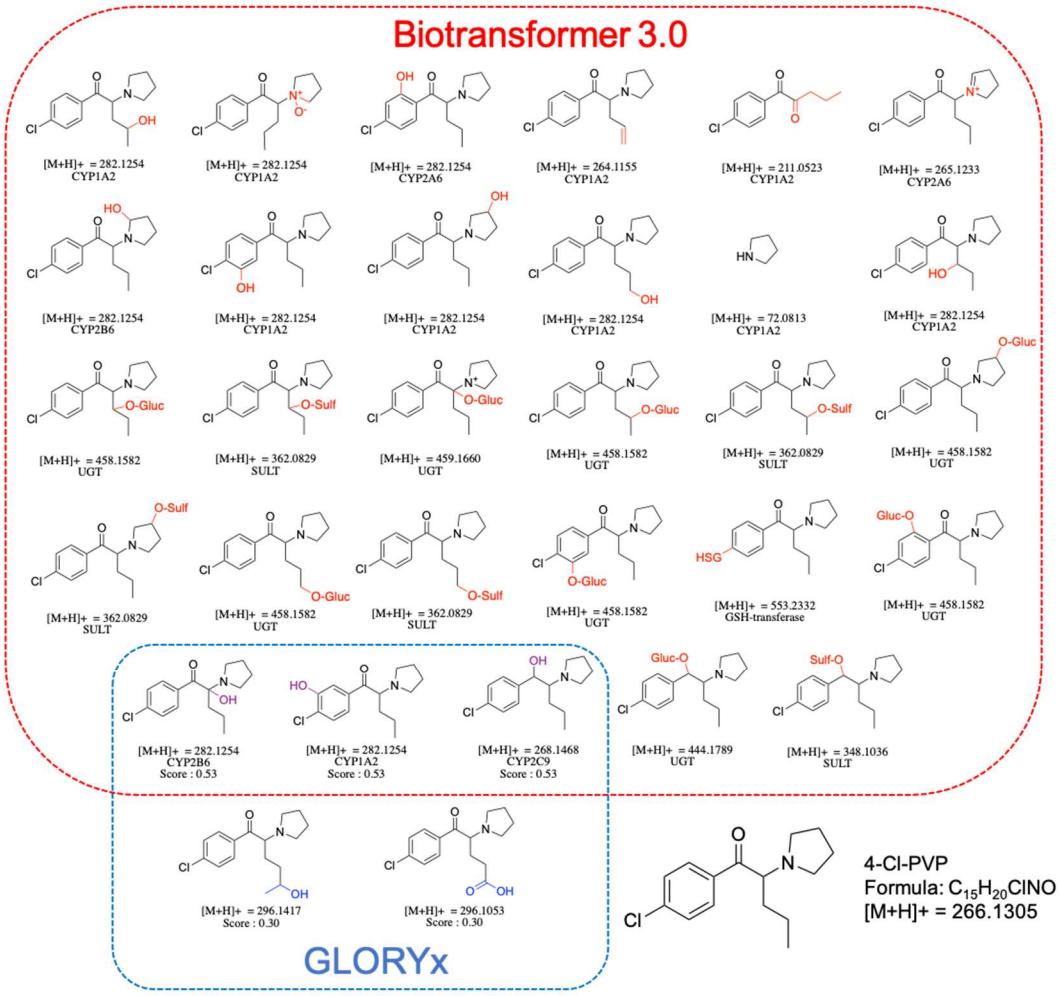

Figure 3: *In silico* prediction of 4-Cl-PVP metabolites by GLORYx and BT3 programs, showing the molecular mass [M+H]+, the confidence score (GLORYx), and the cytochromes most likely to be involved in biotransformation reactions (BT3 suggested 29 metabolites, while GLORYx suggested only 5).

AN IN VIVO METABOLIC STUDY OF HUMAN BIOLOGICAL SAMPLES

We studied the *in vivo* metabolism 4-Cl-PVP in human blood and urine samples in a context of intoxication. The urine and plasma 4-Cl-PVP concentrations were respectively 34.4 and 1018.6 µg/L on admission and 7.4 and 213.1 µg/L 24 hours after admission. Using molecular networking, we found 13 compounds structurally related to 4-Cl-PVP and with mass shifts that might correspond to biotransformations – making them putative metabolites (Figure 4, Table 1). This approach enabled the semiquantitative visualization of how the molecules were distributed in the two matrices. All the potential metabolites were present at higher concentrations in urine samples than in blood samples.

The most intensely detected putative metabolites were the ions *m/z* 282.1254 (monohydroxylated derivatives) and *m/z* 298.1204 (dihydroxylated derivatives). We confirmed the presence of five putative metabolites predicted by our *in vitro* or *in silico* models: *m/z* 280.1097 (RT: 8.4 min), *m/z* 282.1254 (RT: 7.0 min), *m/z* 282.125 (RT: 7.8 min), *m/z* 314.1153 (RT: 6.0 min), and *m/z* 298.1204 (RT: 6.2 min). We also identified glucuronoconjugated phase II metabolites, as highlighted by a mass shift of 176.033. Using information propagation, we suggest that the ions *m/z* 456.1418, *m/z* 458.1574, *m/z* 472.1366, *m/z* 474.1524 and *m/z* 490.1472 are glucuronoconjugated derivatives of the ions found *in vitro* with *m/z* 280.1097, *m/z* 282.1254, *m/z* 296.1047, *m/z* 298.1204, *m/z* 300.1367 and *m/z* 314.1153, respectively (Figure 4).

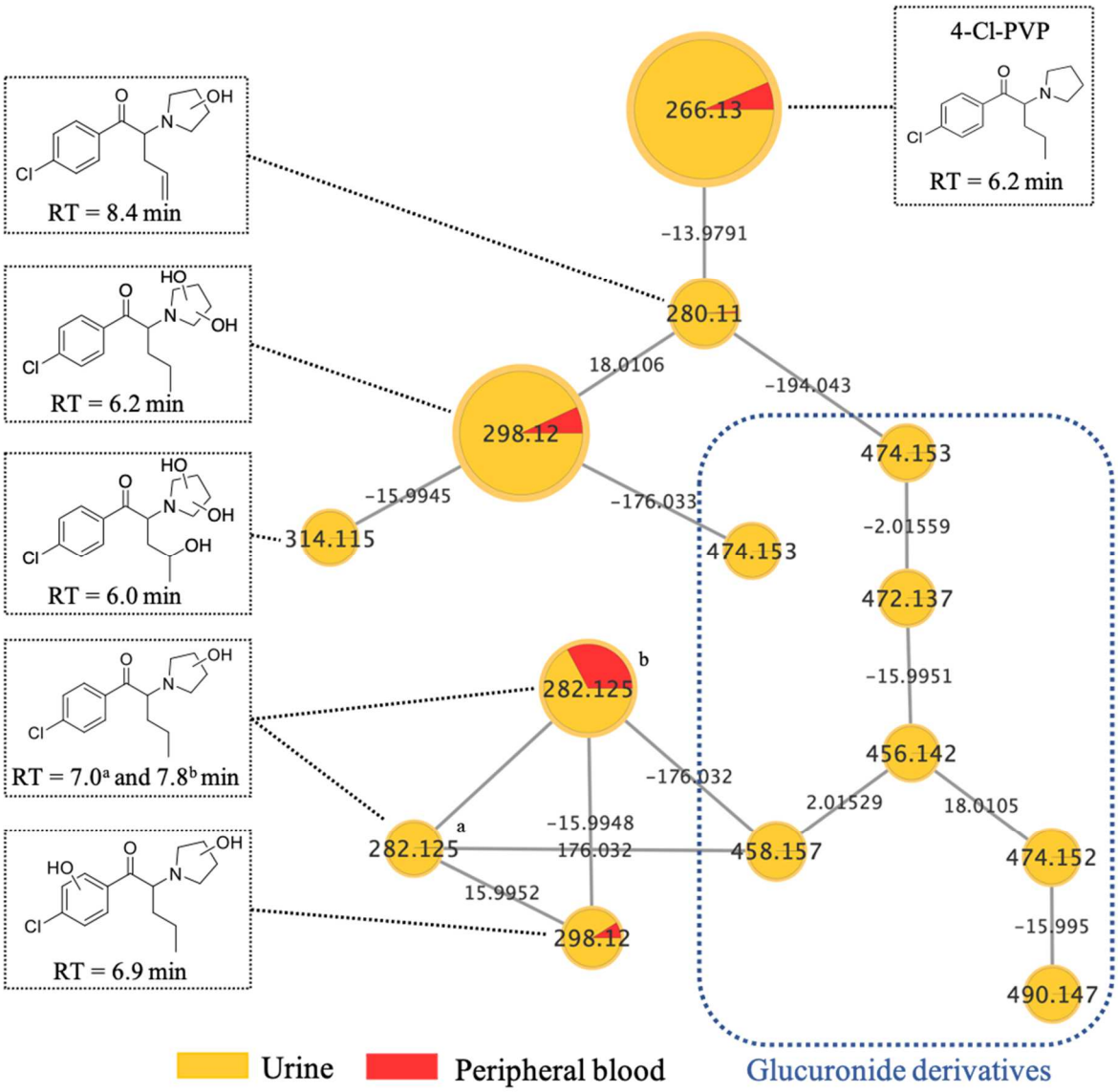

Figure 4: Molecular network of metabolites of 4-Cl-PVP in vivo in urine (yellow) and peripheral blood (red) on admission. Nodes are labeled with the exact protonated mass (m/z), and the links are labeled with the exact mass shift. Candidate 4-Cl-PVP metabolites are linked to the corresponding nodes. RT: retention time (in minutes). Isomers with different retention times are labelled with letters (a and b) to distinguish them.

SUMMARY OF THE IN VITRO, IN VIVO AND *IN SILICO* DATA

Our present *in vitro, in vivo* and *in silico* data and the literature data on 4-Cl-PVP metabolism are summarized in Table 1 (Lopes et al. 2021). Isomers such as hydroxylated-4-Cl-PVP-derivatives were separated and labelled by letters, as a function of the RT. As observed previously, we found that (i) *in vitro* and human sample analyses gave similar results, and (ii) the metabolites identified *in vitro* were found much more frequently in the patient's urine samples than in the patient's blood samples (Gicquel et al. 2021a). This comparison highlighted interesting 4-Cl-PVP consumption markers because the molecules were found in the various models and had a high intensity in HRMS (ions with *m/z* 282.1254 and *m/z* 298.1204). We also summarize these putative metabolites within possible metabolism pathways within Figure 5.

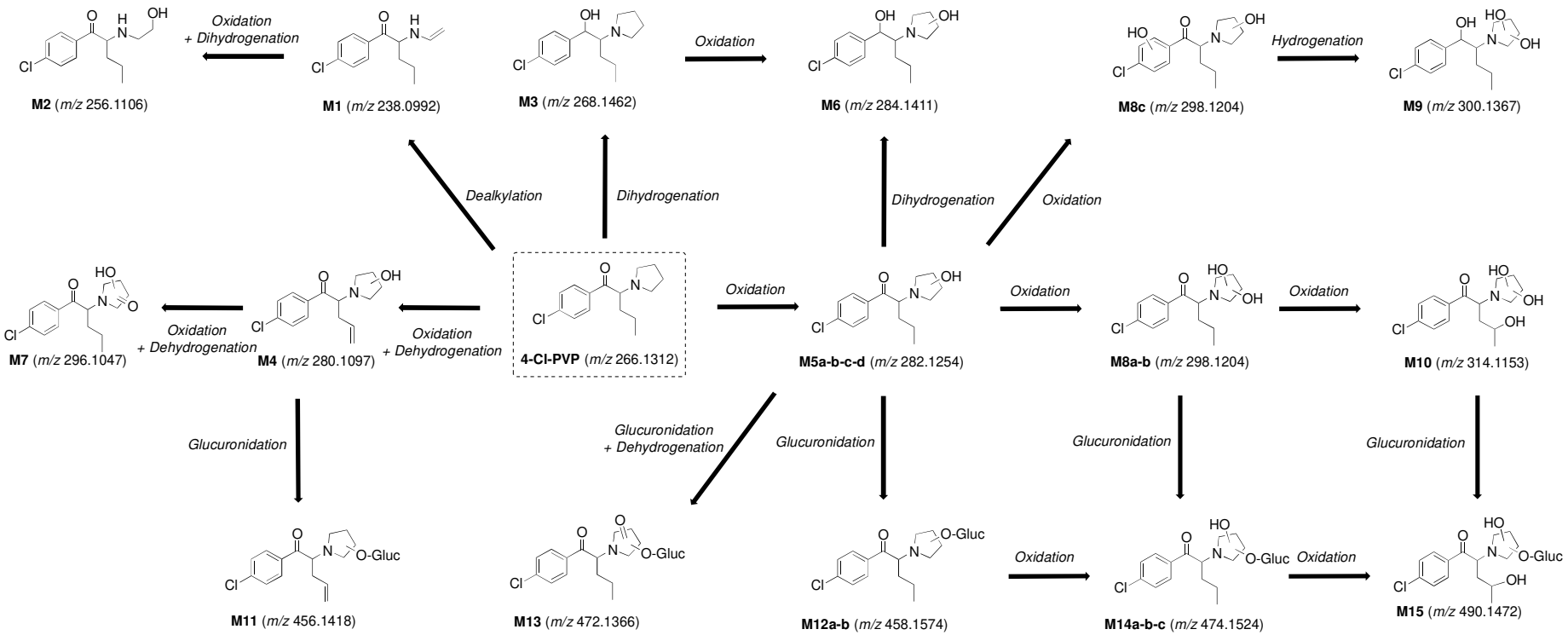

Figure 5 Proposed metabolites of 4-Cl-PVP structures and postulated biotransformation combining both human and in vitro studies

Discussion

The objectives of the study were (i) to elucidate the metabolism of 4-Cl-PVP by applying a combination of *in vitro, in vivo* and *in silico* techniques, and (ii) to was to identify putative 4-Cl-PVP additional consumption markers for use in clinical practice.

Using a combination of *in vitro*, *in vivo* and *in silico* approaches, we identified 15 potential metabolites of 4-Cl-PVP, 10 of which had not been described previously. Our study of the kinetics of metabolism *in vitro* provided valuable insights into the nodes linked to 4-Cl-PVP. The concomitant metabolism of 4-Cl-PVP and the appearance of structurally related molecules suggests strongly that the latter were metabolites – none of which were detected in the culture medium in the absence of 4-Cl-PVP. Furthermore, the putative intermediate and final metabolites provide a better understanding of the steps in the metabolism of 4-Cl-PVP. Nevertheless, in the absence of commercial standards for each metabolite, the fragments analysis with SIRIUS 4.0 software yielded putative structures rather than proven chemical structures (Schymanski et al. 2014).

The comparison of *in vitro* data with *in vivo* data was of particular interest. Indeed, several *in vivo* metabolites were found *in vitro*, suggesting that our cellular model is relevant and that we can have a high degree of confidence in these putative metabolites. Moreover, the good ionization response of the ions *m/z* 282.1254 and *m/z* 298.1204 (evidenced by the large nodes obtained in the molecular networks *in vitro* and *in vivo*) suggests that mass spectrometry detection is sensitive. These elements prompt us to suggest that both compounds are 4-Cl-PVP additional consumption markers. We also identified many isomers (especially hydroxylated derivatives) on the basis of differences in the fragmentation spectrum and RT. However, further studies of additional biological samples would be needed to discriminate between the metabolites found in cell models but not in our patient.

In vivo, the analysis of urine samples allowed us to identify a number of glucuronoconjugated 4-Cl-PVP derivatives (*m/z* 456.1418, *m/z* 458.1574, *m/z* 472.1366, *m/z* 474.1524 and *m/z* 490.1472); these derivatives appeared later than the phase I metabolites and thus extended the detection time window for this NPS. This hypothesis is also supported by the fact that a greater number of phase II metabolites

are detected in *in vivo* samples than in *in vitro* samples. Hence, these experiments provided valuable pharmacokinetic data on 4-Cl-PVP and its metabolites and showed that urine is the matrix of choice when seeking to diagnose 4-Cl-PVP intoxication. In this context, the analysis of a serial urine samples would provide precise data on the detection time windows for these compounds. In addition to identifying these consumption markers, we quantified 4-Cl-PVP in human blood and urine samples at two different timepoints (upon admission to the ICU and 24 hours after) for the first time and thus were able to estimate toxic concentrations of 4-Cl-PVP in these matrices.

Of the 31 metabolites predicted *in silico*, only hydroxylated (*m/z* 282.1254) and glucuronoderivated metabolites (*m/z 458.1575)* were found in the *in vitro* and *in vivo* models. However, the BT3 software predicts sulfoconjugate derivatives not found in humans and in vitro, while these derivatives have already been detected for other molecules by the molecular network (Allard et al. 2020). Also, the prediction of cytochrome by the BT3 software seems to us sometimes erroneous, it is in particular the case for the predicted metabolite *m/z* 268.1468 probably reduced by an alcohol dehydrogenase rather than the CYP2C9. Thus, metabolism prediction software appears to have little relevance for cathinone derivatives, as previously described by Carlier *et al.* (2022) for 3-fluoro-alpha-pyrrolidinovalerophenone (3-F-αPVP) (Carlier et al. 2022). More broadly, these observations call for caution in the interpretation of metabolic data generated by these software tools. Given that these software tools feature machine learning, one can assume that the limited amount of data on the metabolism of these drugs prevents the accurate prediction of biotransformation reactions from quantitative structure-activity relationships. Thanks to the use of cross-disciplinary approaches, better knowledge of the metabolism of these molecules might help to refine the *in silico* predictions.

Lastly, a comparison of our metabolic results for 4-Cl-PVP with the literature data confirmed the presence of four metabolites previously described by Lopez *et al.* (namely M3 (*m/z* 268.1462), M5d (*m/z* 282.1254), M6 (*m/z* 284.1411) and M12a (*m/z* 458.1574); Table 1) (Lopes et al. 2021). Interestingly, the 4-Cl-PVP biotransformation reactions identified in our study (dehydrogenation, oxidation, oxidation + dehydrogenation, hydrolysis, carboxylation, and glucuronoconjugation) were similar to those reported for other PVP derivatives (Manier et al. 2018; Carlier et al. 2020, 2022).

Conclusion

By using *in vitro*, *in silico* and *in vivo* models and a molecular networking approach, we identified 15 putative 4-Cl-PVP metabolites - 10 of which had not been described previously. These metabolites might be 4-Cl-PVP additional consumption markers with value for hospital toxicology labs. The high intensity of the hydroxy-4-Cl-PVP (*m/z* 282.1254) and dihydroxy-4-Cl-PVP (*m/z* 298.1204) metabolites in *in vivo* and *in vitro* matrices suggests that these two compounds are particularly relevant markers of this NPS. Their inclusion in mass spectrometry identification databases might allow the specific, sensitive detection of 4-Cl-PVP intoxications over a broader time window than for the parent molecule alone.

Acknowledgments

This project was support by financial allowance “Défi Scientifique” Université Rennes 1.

The authors thank David Fraser PhD (Biotech Communication SARL, Ploudalmezeau, France) for copy-editing assistance and Bernard Fromenty (NuMeCan Institute) for his helpful contribution.

Declarations

Competing interests

The authors declare no conflict of interest. The funders had no role in the design of the study; in the collection, analyses, or interpretation of data; in the writing of the manuscript, or in the decision to publish the results.

Ethical standards

The study was conducted according to the guidelines of the Declaration of Helsinki, and approved by the Ethics Committee of University Hospital of Rennes.

BIBLIOGRAPHY

Abuse NI on D (2020) Synthetic Cathinones (“Bath Salts”) DrugFacts. In: Natl. Inst. Drug Abuse. https://nida.nih.gov/publications/drugfacts/synthetic-cathinones-bath-salts. Accessed 25 Jul 2022

Allard S, Allard P-M, Morel I, Gicquel T (2019) Application of a molecular networking approach for clinical and forensic toxicology exemplified in three cases involving 3-MeO-PCP, doxylamine, and chlormequat. Drug Test Anal 11:669–677. https://doi.org/10.1002/dta.2550

Allard S, Le Daré B, Allard P-M, et al (2020) Comparative molecular networking analysis of a Rauwolfia plant powder and biological matrices in a fatal ingestion case. Forensic Toxicol 38:447–454. https://doi.org/10.1007/s11419-020-00531-0

Allibe N, Richeval C, Phanithavong M, et al (2018) Fatality involving ocfentanil documented by identification of metabolites. Drug Test Anal 10:995–1000. https://doi.org/10.1002/dta.2326

Ameline A, Greney H, Monassier L, et al (2019a) Metabolites to parent 3-MeO-PCP ratio in human urine collected in two fatal cases. J Anal Toxicol 43:321–324. https://doi.org/10.1093/jat/bky097

Ameline A, Richeval C, Gaulier J-M, et al (2019b) Detection of the designer benzodiazepine flunitrazolam in urine and preliminary data on its metabolism. Drug Test Anal 11:223–229. https://doi.org/10.1002/dta.2480

Aninat C, Piton A, Glaise D, et al (2006) Expression of cytochromes P450, conjugating enzymes and nuclear receptors in human hepatoma HepaRG cells. Drug Metab Dispos Biol Fate Chem 34:75–83. https://doi.org/10.1124/dmd.105.006759

Batisse A, Eiden C, Deheul S, et al (2022) Chemsex practice in France: An update in Addictovigilance data. Fundam Clin Pharmacol 36:397–404. https://doi.org/10.1111/fcp.12725

Carlier J, Berardinelli D, Montanari E, et al (2022) 3F-α-pyrrolydinovalerophenone (3F-α-PVP) in vitro human metabolism: Multiple in silico predictions to assist in LC-HRMS/MS analysis and targeted/untargeted data mining. J Chromatogr B Analyt Technol Biomed Life Sci 1193:123162. https://doi.org/10.1016/j.jchromb.2022.123162

Carlier J, Diao X, Giorgetti R, et al (2020) Pyrrolidinyl Synthetic Cathinones α-PHP and 4F-α-PVP Metabolite Profiling Using Human Hepatocyte Incubations. Int J Mol Sci 22:230. https://doi.org/10.3390/ijms22010230

de Bruyn Kops C, Šícho M, Mazzolari A, Kirchmair J (2021) GLORYx: Prediction of the Metabolites Resulting from Phase 1 and Phase 2 Biotransformations of Xenobiotics. Chem Res Toxicol 34:286–299. https://doi.org/10.1021/acs.chemrestox.0c00224

Di Trana A, Brunetti P, Giorgetti R, et al (2021) In silico prediction, LC-HRMS/MS analysis, and targeted/untargeted data-mining workflow for the profiling of phenylfentanyl in vitro metabolites. Talanta 235:122740. https://doi.org/10.1016/j.talanta.2021.122740

Diao X, Huestis MA (2019) New Synthetic Cannabinoids Metabolism and Strategies to Best Identify Optimal Marker Metabolites. Front Chem 7:109. https://doi.org/10.3389/fchem.2019.00109

Du Q-S, Huang R-B, Chou K-C (2008) Recent Advances in QSAR and Their Applications in Predicting the Activities of Chemical Molecules, Peptides and Proteins for Drug Design. Curr Protein Pept Sci 9:248–259. https://doi.org/10.2174/138920308784534005

Dührkop K, Fleischauer M, Ludwig M, et al (2019) SIRIUS 4: a rapid tool for turning tandem mass spectra into metabolite structure information. Nat Methods 16:299–302. https://doi.org/10.1038/s41592-019-0344-8

European Monitoring Centre for Drugs and Drug Addiction. (2022) European drug report 2022: trends and developments. Publications Office, LU

Ferron P-J, Le Daré B, Bronsard J, et al (2021) Molecular Networking for Drug Toxicities Studies: The Case of Hydroxychloroquine in COVID-19 Patients. Int J Mol Sci 23:82. https://doi.org/10.3390/ijms23010082

Gertrudes JC, Maltarollo VG, Silva RA, et al (2012) Machine Learning Techniques and Drug Design. Curr Med Chem 19:4289–4297. https://doi.org/10.2174/092986712802884259

Gicquel T, Pelletier R, Richeval C, et al (2021a) Metabolite elucidation of 2-fluoro-deschloroketamine (2F-DCK) using molecular networking across three complementary in vitro and in vivo models. Drug Test Anal. https://doi.org/10.1002/dta.3162

Gicquel T, Richeval C, Mesli V, et al (2021b) Fatal intoxication related to two new arylcyclohexylamine derivatives (2F-DCK and 3-MeO-PCE). Forensic Sci Int 324:110852. https://doi.org/10.1016/j.forsciint.2021.110852

Hugbart C, Verres Y, Le Daré B, et al (2020) Non-oxidative ethanol metabolism in human hepatic cells in vitro: Involvement of uridine diphospho-glucuronosyltransferase 1A9 in ethylglucuronide production. Toxicol In Vitro 66:104842. https://doi.org/10.1016/j.tiv.2020.104842

Kazmi SR, Jun R, Yu M-S, et al (2019) In silico approaches and tools for the prediction of drug metabolism and fate: A review. Comput Biol Med 106:54–64. https://doi.org/10.1016/j.compbiomed.2019.01.008

Kelly JP (2011) Cathinone derivatives: a review of their chemistry, pharmacology and toxicology. Drug Test Anal 3:439–453. https://doi.org/10.1002/dta.313

Klingberg J, Keen B, Cawley A, et al (2022) Developments in high-resolution mass spectrometric analyses of new psychoactive substances. Arch Toxicol 96:949–967. https://doi.org/10.1007/s00204-022-03224-2

La Maida N, Di Trana A, Giorgetti R, et al (2021) A Review of Synthetic Cathinone-Related Fatalities From 2017 to 2020. Ther Drug Monit 43:52–68. https://doi.org/10.1097/FTD.0000000000000808

Le Daré B, Allard S, Bouvet R, et al (2020a) A case of fatal acebutolol poisoning: an illustration of the potential of molecular networking. Int J Legal Med 134:251–256. https://doi.org/10.1007/s00414-019-02062-9

Le Daré B, Ferron P-J, Allard P-M, et al (2020b) New insights into quetiapine metabolism using molecular networking. Sci Rep 10:19921. https://doi.org/10.1038/s41598-020-77106-x

Le Daré B, Ferron P-J, Couette A, et al (2021) In vivo and in vitro α-amanitin metabolism studies using molecular networking. Toxicol Lett 346:1–6. https://doi.org/10.1016/j.toxlet.2021.04.006

Lopes BT, Caldeira MJ, Gaspar H, Antunes AMM (2021) Metabolic Profile of Four Selected Cathinones in Microsome Incubations: Identification of Phase I and II Metabolites by Liquid Chromatography High Resolution Mass Spectrometry. Front Chem 8:609251. https://doi.org/10.3389/fchem.2020.609251

Majchrzak M, Celiński R, Kuś P, et al (2018) The newest cathinone derivatives as designer drugs: an analytical and toxicological review. Forensic Toxicol 36:33–50. https://doi.org/10.1007/s11419-017-0385-6

Manier SK, Richter LHJ, Schäper J, et al (2018) Different in vitro and in vivo tools for elucidating the human metabolism of alpha-cathinone-derived drugs of abuse. Drug Test Anal. https://doi.org/10.1002/dta.2355

Miotto K, Striebel J, Cho AK, Wang C (2013) Clinical and pharmacological aspects of bath salt use: a review of the literature and case reports. Drug Alcohol Depend 132:1–12. https://doi.org/10.1016/j.drugalcdep.2013.06.016

Pelletier R, Le Daré B, Grandin L, et al (2021) New psychoactive substance cocktail in an intensive care intoxication case elucidated by molecular networking. Clin Toxicol Phila Pa 1–4. https://doi.org/10.1080/15563650.2021.1931693

Quesnot N, Bucher S, Gade C, et al (2018) Production of chlorzoxazone glucuronides via cytochrome P4502E1 dependent and independent pathways in human hepatocytes. Arch Toxicol 92:3077–3091. https://doi.org/10.1007/s00204-018-2300-2

Richeval C, Gicquel T, Hugbart C, et al (2017) In vitro Characterization of NPS Metabolites Produced by Human Liver Microsomes and the HepaRG Cell Line Using Liquid Chromatographyhigh Resolution Mass Spectrometry (LC-HRMS) Analysis: Application to Furanyl Fentanyl. Curr Pharm Biotechnol 18:806–814. https://doi.org/10.2174/1389201018666171122124401

Schymanski EL, Jeon J, Gulde R, et al (2014) Identifying small molecules via high resolution mass spectrometry: communicating confidence. Environ Sci Technol 48:2097–2098. https://doi.org/10.1021/es5002105

Seidl B, Schuhmacher R, Bueschl C (2022) CPExtract, a Software Tool for the Automated Tracer-Based Pathway Specific Screening of Secondary Metabolites in LC-HRMS Data. Anal Chem 94:3543–3552. https://doi.org/10.1021/acs.analchem.1c04530

Tyzack JD, Kirchmair J (2019) Computational methods and tools to predict cytochrome P450 metabolism for drug discovery. Chem Biol Drug Des 93:377–386. https://doi.org/10.1111/cbdd.13445

Wagmann L, Frankenfeld F, Park YM, et al (2020) How to Study the Metabolism of New Psychoactive Substances for the Purpose of Toxicological Screenings-A Follow-Up Study Comparing Pooled Human Liver S9, HepaRG Cells, and Zebrafish Larvae. Front Chem 8:539. https://doi.org/10.3389/fchem.2020.00539

Wishart DS, Tian S, Allen D, et al (2022) BioTransformer 3.0-a web server for accurately predicting metabolic transformation products. Nucleic Acids Res gkac313. https://doi.org/10.1093/nar/gkac313

Table 1. Putative metabolites of 4-Cl-PVP found here in vitro*, in vivo, and* in silico*, and in the literature. NA: not applicable; x = presence of the molecule. Metabolite isomers with different retention times are labeled with letters to distinguish them.*

									In vitro	***In vivo***		***In silico***		**Reference**
Molecule	**[M+H]+ in theory**	**[M+H]+ observed**	**Formula**	**RT (min)**	**Biotransformation reactions**	**Mass shift**	**Δppm**	**Main fragments [M+H]+**	**HepaRG cells**	**Urine**	**Blood**	**BT3**	**GLORYx**	Mentioned in (Lopes et al. 2021)
Parent	266.1312	266.1305	C15H20ClNO	6.2	None	NA	-2.6	195.0577 138.9949 125.0157	x	x	x	x	x	x
M1	238.0992	238.0990	C13H16ClNO	6.0	Demethylation x2	-28.0313	-0.8	195.0577 152.0019 125.0157	x					
M2	256.1106	256.1094	C13H18ClNO2	5.9	Demethylation x2 + Oxidation + Dihydrogenation	-10.0211	-4.7	195.0577 153.0101 125.0157	x					
M3	268.1462	NA	C15H22ClNO	NA	Dihydrogenation	+2.0157	NA	NA				x	x	x
M4	280.1097	280.1097	C15H18ClNO2	8.4	Oxidation + Dehydrogenation	+13.9792	0.0	195.0577 138.9949 125.0157	x	x	x			

M5a	282.1254	282.1252	C15H20ClNO2	6.0	Oxidation	+15.9949	-0.7	195.0577 138.9949 125.0157	x					
M5b	282.1254	282.1249	C15H20ClNO2	7.0	Oxidation	+15.9949	-1.8	179.0621 144.0933 98.0604		x	x	x	x	
M5c	282.1254	282.1253	C15H20ClNO2	7.8	Oxidation	+15.9949	-0.4	179.0621 144.0933 98.0604		x	x			
M5d	282.1254	NA	C15H20ClNO2	NA	Oxidation	+15.9949	NA	264.1155 142.1233 153.0109						x
M6	284.1411	284.1409	C15H22ClNO2	6.2	Oxidation + Dihydrogenation	+18.0106	-0.7	194.0730 152.0261 125.0153	x					x
M7	296.1047	296.1043	C15H18ClNO3	7.5	Oxidation x2 + Dehydrogenation	+29.9742	-1.4	195.0577 138.9949 125.0157	x				x	
M8a	298.1204	298.1197	C15H20ClNO3	6.2	Oxidation x2	+31.9899	-2.3	280.1096 194.0730	**x**	**x**	**x**			

								125.0151						
M8b	298.1205	298.1201	C15H20ClNO3	6.9	Oxidation x2	+31.9900	-1.0	280.1097 179.0621 125.0153		x	x			
M8c	298.1206	298.1197	C15H20ClNO3	7.4	Oxidation x2	+31.9901	-2.3	212.0834 194.0730 125.0153	x					
M9	300.1367	300.1356	C15H22ClNO3	5.8	Oxidation x2 + Dihydrogenation	+34.0055	-1.3	206.0728 194.0729 125.0152	x					
M10	314.1153	314.1146	C15H20ClNO4	6.0	Oxidation x3	+47.9848	-2.2	296.1044 206.0729 125.0152	x	x	x			
M11	456.1418	456.1419	C21H26ClNO8	7.3	Oxidation + Dehydrogenation + Glucuronidation	+190.0113	0.2	280.1096 262.0999 179.0621		x	x			
M12a	458.1574	458.1558	C21H28ClNO8	5.7	Oxidation + Glucuronidation	+192,0269	-3.5	282.1251 138.9942 125.0152	x	x	x	x		x
M12b	458.1574	458.1572	C21H28ClNO8	7.0		+192.0269	-0.4	264.1145		x	x			

					Oxidation + Glucuronidation			179.0620 98.0603						
M13	472.1366	472.1370	C21H26ClNO9	5.6	Carboxylation + Glucuronidation	+206.0061	0.8	278.0940 195.0570 125.0153		x	x			
M14a	474.1524	474.1526	C21H28ClNO9	5.3	Oxidation x2 + Glucuronidation	+208.0218	0.6	280.1098 195.0570 125.0154		x	x			
M14b	474.1524	474.1527	C21H28ClNO9	5.8	Oxidation x2 + Glucuronidation	+208.0219	0.8	280.1098 125.0154 87.0445		x	x			
M14c	474.1524	474.1524	C21H28ClNO9	6.9	Oxidation x2 + Glucuronidation	+208.0220	0.2	280.1098 196.0888 179.0612		x	x			
M15	490.1472	490.1474	C21H28ClNO10	6.6	Oxidation x3 + Glucuronidation	+224.0167	0.4	296.1046 196.0888 85.0289		x				